

Simulated NEMA NU2 Performance of the Ultra-Compact Clinical NeuroLF Brain PET

E. Mikhaylova, M. Jehl, D. Deidda, K. Thielemans, V. Dao, M. Ahnen and J. Fischer

Abstract— A new clinical brain positron emission tomography (PET) scanner NeuroLF with octagonal detector arrangement is being finalized. Image reconstruction and data correction methods adapted for non-cylindrical scanner geometry were recently added to the open-source Software for Tomographic Image Reconstruction (STIR). We first evaluate the performance of the NeuroLF following NEMA NU2-2018. Second, the results are compared to our earlier brain PET system prototype BPET. Finally, the newly adapted STIR image reconstruction methods are validated. For this purpose, NEMA tests were performed on NeuroLF simulations using the GATE software. The results were processed with STIR using the “Cylindrical” scanner geometry class and using the new “BlocksOnCylindrical” class. Spatial resolution close to the field-of-view center is estimated to improve from $4.0 \times 3.9 \times 3.5$ mm³ for the BPET prototype scanner to $2.12 \times 2.20 \times 2.42$ mm³ and $2.33 \times 2.32 \times 3.19$ mm³ for the NeuroLF scanner after processing data with “BlocksOnCylindrical” and “Cylindrical” scanner geometry classes correspondingly. Total sensitivity using an energy window of [425 keV, 650keV] at the field-of-view center is estimated to improve from 2.9 cps/kBq (BPET) to 5.76 cps/kBq (“BlocksOnCylindrical”) and 5.65 cps/kBq (“Cylindrical”) for NeuroLF. The contrast recovery of the 4.5-mm-diameter rod of an image quality phantom is estimated to improve from 0 (BPET) to 45% (“BlocksOnCylindrical”) and 36% (“Cylindrical”) for NeuroLF. We show further comparisons on the peak noise-equivalent count rate. The obtained results validate the new STIR image reconstruction methods and support the performance evaluation of NeuroLF.

Index Terms— BlocksOnCylindrical, Brain PET, NEMA NU2-2018, Simulation, STIR 5.0.0

I INTRODUCTION

AFTER characterizing the performance of the earlier developed ultra-compact brain PET prototype BPET [1] and performing the clinical trial [2], the next generation clinical brain PET system NeuroLF features were optimized. Currently, NeuroLF system development is being finalized. Performance testing using the NEMA NU2-2018 protocol [3] is scheduled in the near future. At the same time, we enhanced the Software for Tomographic Image Reconstruction (STIR) [4] and released a new software version 5.0.0 where the majority of data processing, image reconstruction and data correction methods

E. Mikhaylova (e-mail: ekaterina.mikhaylova@positrigo.com), M. Jehl (e-mail: markus.jehl@positrigo.com), M. Ahnen (e-mail: max.ahnen@positrigo.com) and J. Fischer (jannis.fischer@positrigo.com) are with Positrigo AG, Zurich, 8005 Switzerland.

D. Deidda is with National Physical Laboratory, Teddington, TW11 0LW UK (e-mail: daniel.deidda@npl.co.uk).

K. Thielemans is with 1) Algorithms and Software Consulting Ltd, London, UK, and 2) Institute of Nuclear Medicine, University College London, UK (e-mail: kris@asc.uk.com)

V. Dao is with Leeds Institute of Cardiovascular and Metabolic Medicine, University of Leeds, West Yorkshire, LS9JT UK, (e-mail: V.A.Dao@leeds.ac.uk).

were adapted and tested for a non-cylindrical prism-like PET scanner geometry [5,6]. In this work we make a preliminary comparison between the upcoming NeuroLF brain PET system simulated with GATE [7] with the measured BPET prototype system performance. Additionally, we used the simulated data to validate the adapted prism-geometry scanner STIR class framed “BlocksOnCylindrical”.

Table I compares main geometrical and electronic features of the prototype brain scanner BPET and the 1st generation clinical brain system NeuroLF (real and simulated).

TABLE I
BPET AND NEUROLF COMPARISON

	BPET [1]	NeuroLF PRELIMINARY, simulated, planned
Detector arrangement	Octagon	Octagon
Crystal material	LYSO	LYSO
Crystal size, mm ³	4.1×4.1×10	3.19×3.19×10 ^a
Crystal array	6 × 6	4 × 4
SIPM size, mm ²	3 × 3	4 × 4
Light sharing	4:1	4:1
Energy resolution	14.2%	13.5%
Considered energy window	425 – 650	425 – 650
Coincidence timing resolution (CTR)	4 ns	600 ps
Considered coincidence time window	8 ns	1.8 ns
Scanner axial field-of-view, mm	128.4	163.2
Scanner inner diameter crystal surface, flat-to-flat, mm	254.52	266

^aThere will be 3 variants of the system available: with 10-, 15, and 20-mm-long crystals. In this work we simulate the 10 mm version.

II MATERIAL AND METHODS

The GATE simulations are performed with the 10-mm-long crystals NeuroLF variant. All simulations, except for the image quality test, accurately match the measurements procedures described in the NEMA NU2-2018 standard protocol. Time-of-Flight (TOF) was out-scoped for now.

For the image quality test, the phantom described in [8] was placed into the NeuroLF field-of-view (FOV). The phantom is an acrylic cylinder filled with ¹⁸F radioactive water of 51.6 MBq total activity. The length is 103 mm and the diameter is 135 mm. Inside there is an insert with 6 rods of 50 mm in the length and various diameters (20, 15, 12, 9, 6, 4.5 mm) filled with air, non-radioactive and radioactive water. The phantom active rod-to-background activity concentration is 4-to-1. The image was reconstructed with the Maximum Likelihood Expectation Maximization (MLEM) algorithm using 40 iterations. The data were corrected for gamma attenuation, randoms and scatters. The image analysis was performed according to NEMA NU2-2018.

III RESULTS

A. Spatial Resolution

According to NEMA NU2-2018 the point source should be reconstructed with the Filtered Backprojection (FBP) method. However, a “BlocksOnCylindrical” implementation of FBP is not yet available in STIR. Therefore, the data were reconstructed with 5 MLEM iterations. Table II summarizes the results. The FBP result was also added for completeness.

TABLE II
NEMA NU2-2018 SPATIAL RESOLUTION RESULTS

NeuroLF. Simulated data. Radial, tangential, axial (mm)			
Source position, mm	5 iter. MLEM “BlocksOnCyl.”	5 iter. MLEM “Cylindrical”	FBP2D “Cylindrical”
A=0, R=10	2.12, 2.20, 2.42	2.33, 2.32, 3.19	2.90, 3.05, 2.27
A=0, R=100	4.35, 3.33, 2.65	4.32, 4.27, 3.31	4.69, 5.18, 3.53
A=X, R=10	2.10, 2.19, 2.16	2.30, 2.30, 3.28	2.91, 3.07, 2.83
A=X, R=100	4.71, 2.98, 2.42	4.49, 3.92, 3.32	4.44, 5.60, 3.39
BPET. Measured data [1]. Radial, tangential, axial (mm)			
A=0, R=10	-	-	4.0, 3.9, 3.5
A=0, R=100	-	-	4.2, 3.7, 3.6
A=X, R=10	-	-	3.6, 8.9, 5.3
A=X, R=100	-	-	3.7, 8.3, 5.3

“A” stands for axial position. “R” is for radial position. “X” is for 3/8 axial field-of-view.

B. Counting Rates, Scatter Fraction and Sensitivity

The peak noise-equivalent count rates (NECR), scatter fraction and sensitivity for three different cases are shown in Table III. The sensitivity is calculated after the subtraction of randoms, assuming a central NEMA-NU2 sensitivity line source. In the performance evaluation of BPET, the system showed deficiencies in the count rate performance due to dead time. The goal of the NeuroLF system development is to overcome those. Therefore, the count rate performance simulation for NeuroLF is shown, but not compared to BPET.

TABLE III
NEMA NU2-2018 COUNTING RATE RESULTS

NeuroLF. Simulated data.		
	“BlocksOnCyl.”	“Cylindrical”
$R_{NEC,peak}$, counts/s	23936 @ 80 MBq	22634 @ 80MBq
Scatter Fraction, %	36.1%	36.9%
Total Sens., cps/kBq	5.76	5.65
BPET. Measured data [1].		
Scatter Fraction	-	47%
Total Sens., cps/kBq	-	2.9

C. Contrast Recovery

Figure 1 compares the reconstructed image quality phantom [8] for the simulated NeuroLF acquisition. Table IV compares the corresponding percent contrast for each of hot rod.

IV CONCLUSIONS

The obtained results show a potential of the NeuroLF scanner to significantly improve the counting and imaging performance when compared to the prototype BPET. The results also validate the newly adapted support for non-

cylindrical scanner geometries in the image reconstruction and data correction methods implemented in STIR 5.0.0. The approach to construct sinograms (“BlocksOnCylindrical” or “Cylindrical”) affects not only the final image quality but the counting performance of a PET system. The current results are obtained with 10-mm-long crystals. We expect an improvement in counting performance for the 15-mm- and 20-mm-long crystals.

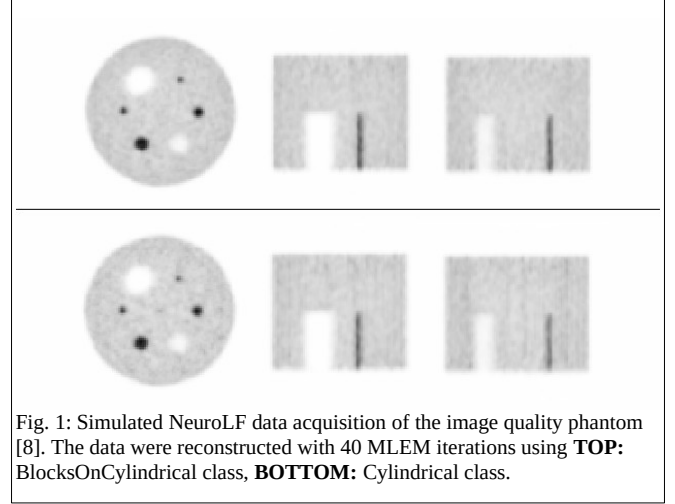


Fig. 1: Simulated NeuroLF data acquisition of the image quality phantom [8]. The data were reconstructed with 40 MLEM iterations using **TOP:** BlocksOnCylindrical class, **BOTTOM:** Cylindrical class.

TABLE IV
NEMA NU2-2018 PERCENT CONTRAST RESULTS

Contrast / Background variability			
Hot rod Diameter	NeuroLF “BlocksOnCyl.”	NeuroLF “Cylindrical”	BPET (meas. [6]) “BlocksOnCyl.”
12 mm	92% / 4.2%	90% / 4.6%	54% / 2.2%
9 mm	81% / 4.9%	74% / 5.2%	28% / 2.2%
6 mm	62% / 6.0%	55% / 6.1%	16% / 2.2%
4.5 mm	45% / 6.5%	36% / 6.8%	invisible

REFERENCES

- [1] M. L. Ahnen *et al.*, “Performance of the Ultra-Compact Fully Integrated Brain PET System BPET,” *2020 IEEE Nuclear Science Symposium and Medical Imaging Conference (NSS/MIC)*, 2020, pp. 1-4, doi: 10.1109/NSS/MIC42677.2020.9508026.
- [2] E. Mikhaylova *et al.*, “The First Clinical Trial of the Ultra-Compact Fully Integrated Brain PET System BPET,” *Eur J Nucl Med Mol Imaging*, 48 (Suppl 1): S1-S648, 2021.
- [3] Performance measurements of positron emission tomographs, NEMA Standards Publication NU 2-2018, Rosslyn, 2018.
- [4] K. Thielemans *et al.*, “STIR: Software for Tomographic Image Reconstruction Release 2,” *Phys Med Biol*, 57 (4), 867-883, 2012, <https://doi.org/10.1088/0031-9155/57/4/867>.
- [5] P. Khateri, J. Fischer, W. Lustermann *et al.*, “Implementation of cylindrical PET scanners with block detector geometry in STIR,” *EJNMMI Phys* 6, 15, 2019, <https://doi.org/10.1186/s40658-019-0248-9>.
- [6] V. Dao *et al.*, “Evaluation of STIR Library Adapted for PET Scanners With Non-Cylindrical Geometry,” *J. Imaging MDPI*, to be published.
- [7] Jan S, Santin G, Strul D *et al.*, “GATE: a simulation toolkit for PET and SPECT,” *Phys Med Biol*, 49(19):4543-4561, 2004, doi:10.1088/0031-9155/49/19/007.
- [8] L. Moliner *et al.*, “NEMA Performance Evaluation of CareMiBrain dedicated brain PET and Comparison with the whole-body and dedicated brain PET systems,” *Sci Rep*, 9, 15484, 2019, <https://doi.org/10.1038/s41598-019-51898-z>.